

The vibrational spectrum of solid ferrocene by inelastic neutron scattering

E. Kemner,^{a)} I. M. de Schepper, and G. J. Kearley

Interfaculty Reactor Institute, Delft University of Technology, Mekelweg 15, 2629 JB Delft, The Netherlands

U. A. Jayasooriya

School of Chemical Sciences, University of East Anglia, Norwich NR4 7TJ, United Kingdom

(Received 18 January 2000; accepted 30 March 2000)

We calculate the spectrum of internal vibrations of a single ferrocene $\text{Fe}(\text{C}_5\text{H}_5)_2$ molecule using *ab initio* density functional theory (without free parameters) and compare this with inelastic neutron scattering data on ferrocene in the solid state at 28 K. Due to the good agreement, we can assign each vibrational mode to each observed peak in the neutron spectrum and so remove ambiguities existing in the literature. There is also consistency between the calculated potential energy of a single ferrocene molecule for different orientations, φ , of the two cyclopentadienyl C_5H_5 rings with respect to each other, which shows a potential barrier of 0.9 kcal/mol, and electron diffraction, and between the calculated shallow minimum at $\varphi=9$ deg and x-ray diffraction. © 2000 American Institute of Physics. [S0021-9606(00)50424-3]

INTRODUCTION

The ferrocene molecule $\text{Fe}(\text{C}_5\text{H}_5)_2$ has attracted much experimental and theoretical interest during the last 40 years.^{1–10} The interest lies in the unusual symmetric form of ferrocene (two identical cyclopentadienyl C_5H_5 rings on both sides of the Fe atom) while it is also the stablest member of the metallocene group, which in general has important catalytic properties. The vibrational frequencies of ferrocene have been calculated theoretically before and verified experimentally by Raman and infrared (IR) spectroscopy. We note that only the frequencies of the lines in the Raman and IR spectra can be accurately calculated, but not their relative intensities. So far reliable intensities could not be obtained from *ab initio* calculations¹¹ since these are indirectly determined by subtle changes in the electron density caused by the vibrations of the nuclei. Therefore, due to a lack of a complete theoretical spectrum, ambiguities easily occur in the assignment of the character of the vibrational mode to the lines observed in the experimental spectra, as discussed, e.g., in Ref. 1.

Here we show for the first time that a full comparison can be made between spectra for ferrocene obtained from inelastic neutron scattering (INS) and theoretical *ab initio* calculations, i.e., including relative intensities. Since neutrons probe the vibrations of the nuclei directly, a theoretical calculation of intensities in the corresponding INS spectrum is feasible. Thus, since both agree, we can unambiguously assign the character of the vibrations to each line in the INS spectrum, as we will do in this paper for the most prominent lines. As a result we can remove some ambiguities existing in the literature.

EXPERIMENT AND RESULTS

The INS neutron spectrum, i.e., the scattered neutron intensity, of ferrocene is obtained as a function of the energy transfer [$S(\omega)$], using the time focused crystal analyser (TFXA) spectrometer at ISIS, United Kingdom.¹² This spectrometer has an indirect geometry and uses a pyrolytic graphite (002) crystal to select a final neutron energy of 24 cm^{-1} . We note that the momentum transfer, Q , is not constant, but varies as $\sqrt{\omega}$. For simplicity we will use $S(\omega)$ to mean $S(Q, \omega)$. This spectrometer has an energy resolution of 2%–4%, depending slightly on the energy transfer. The accessible energy (ω) range is 20–4000 cm^{-1} . The powdered ferrocene sample was contained in an aluminum sample holder and cooled to 28 K. The spectrum of each detector tube is converted to $S(\omega)$ using standard programs. The individual spectra are then added to provide a single spectrum. The result for $S(\omega)$ is shown in Fig. 1.

The calculations are carried out using density functional theory (DFT) on a single ferrocene molecule with the module Dmol³ of the program Cerius².¹³ We use the local density approximation, Perdew Wang functionals, the DND basis set,¹³ and an atomic cutoff radius of 4.95 Å. To determine the shape of the molecule from first principles we calculate the energy $E(\varphi)$ of ferrocene for different orientations φ of the two C_5H_5 rings with respect to each other. Here $\varphi=0$ refers to the state where the atoms of the upper C_5H_5 ring are just on top of the corresponding atoms in the lower ring. This is called the “prismatic”¹⁴ or “eclipsed” orientation. The angle $\varphi=36$ deg refers to the “antiprismatic” or “staggered” orientation, where the atoms in the upper ring are just between the corresponding atoms in the lower ring. First we optimize the positions of the atoms in the eclipsed orientation ($\varphi=0$). We find for the bond lengths: 1.423 Å (CC), 1.093 Å (CH), and 2.027 Å (FeC). We find the H atoms to be tilted 1.6° from the C_5 ring toward the Fe atom. These results agree with those in the literature.^{1,2} We then calculate the energy $E(\varphi)$ for different angles φ using these values for

^{a)} Author to whom correspondence should be addressed; electronic mail: kemner@iri.tudelft.nl

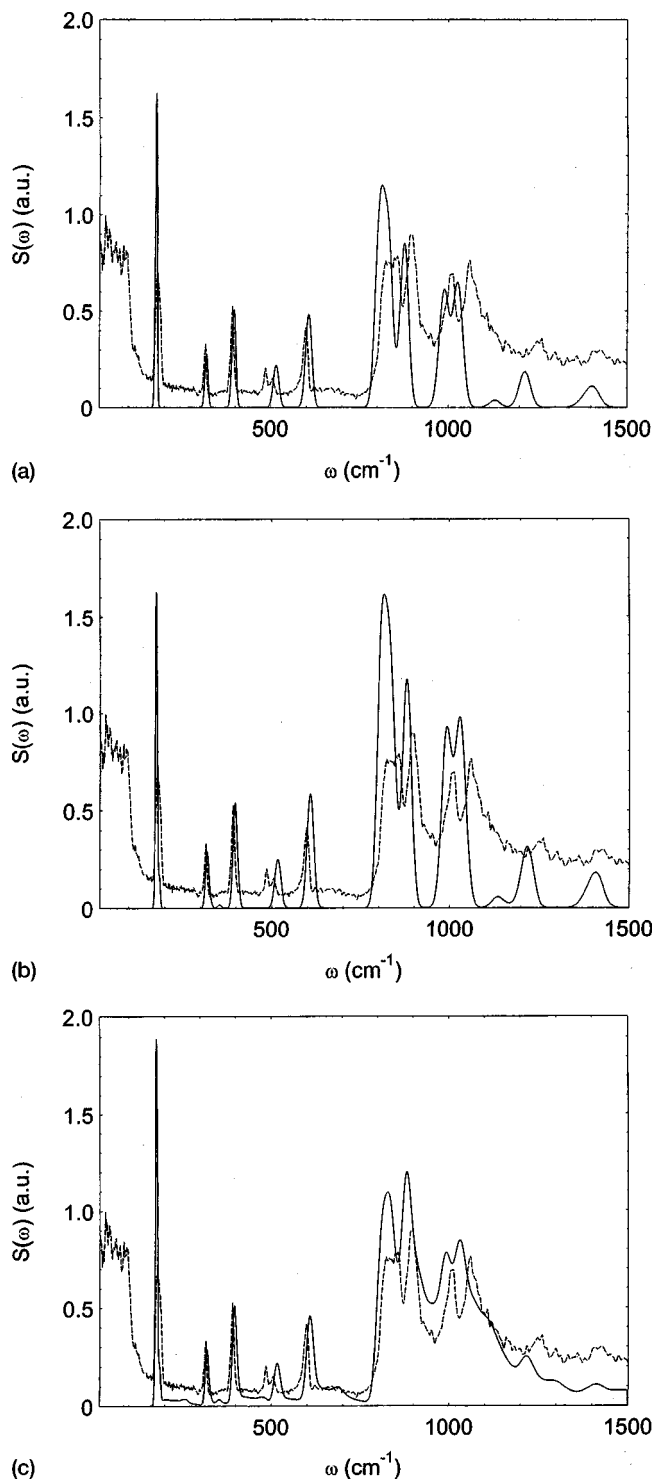


FIG. 1. Inelastic neutron scattering spectrum $S(\omega)$ for solid ferrocene at 28 K (dashed line) compared with DFT calculations on a single ferrocene molecule (solid line) taking into account (a) only the fundamental vibrational modes, (b) the fundamental modes plus overtones and combinations, and (c) fundamental modes, overtones and combinations, and phonons, as explained in the text.

the bond lengths and CH tilt, using the DFT program as discussed above.

The result for $E(\varphi)$ is shown in Fig. 2. The energy is clearly lower for the eclipsed ($\varphi=0$) than for the staggered orientation ($\varphi=36$ deg), although the potential barrier of 0.9 kcal/mol is small, being virtually the same as has been de-

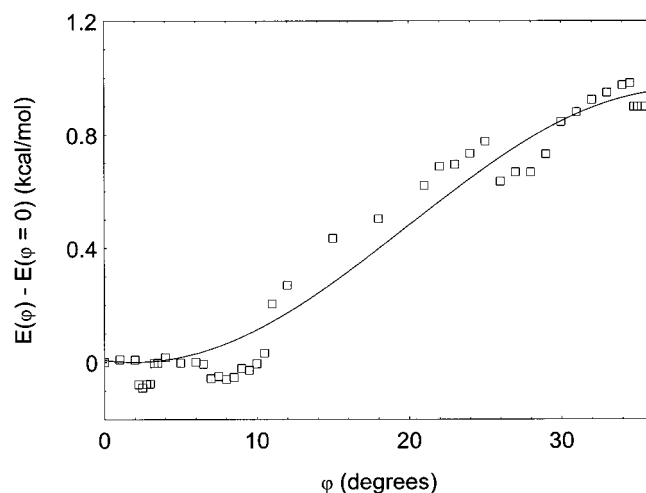


FIG. 2. Internal potential $E(\varphi)$ for rotation of the two C_5H_5 rings in the ferrocene $Fe(C_5H_5)_2$ molecule with respect to each other according to DFT calculations as a function of orientation φ , where $\varphi=0$ corresponds to the eclipsed orientation (open squares). Also shown is a fit with $E(\varphi)=a(1-\cos(\pi(\varphi-b)/36))$, with amplitude $a=0.47$ kcal/mol and phase $b=1.96$ deg (solid line).

rived before from electron diffraction (0.9 ± 0.3 kcal/mol) on ferrocene in the gas phase.³ There are several shallow minima in $E(\varphi)$ which are grouped around $\varphi=0$ and extend up to about 12 deg, which could be artefacts of the numerical calculations. The overall shape of the potential barrier closely resembles a cosine, as shown in Fig. 2. For further calculations we take the rings of the ferrocene molecule as rotated by 9 deg from the eclipsed orientation, to agree with x-ray diffraction on the low-temperature phase of solid ferrocene.² We optimize in this orientation the geometry of the ferrocene molecule again, but find no differences in bond lengths and CH tilt from the eclipsed configuration as given above. Using the so-determined shape of ferrocene we calculate the vibration frequencies of the normal modes and the displacements of all the atoms for each of these modes. These results are taken as input for the program CLIMAX, which converts the data to a theoretical inelastic neutron scattering spectrum $S(\omega)$.¹⁴ CLIMAX has been devised to include the overtones and combinations (due to multiple excitations) and external lattice modes (phonons) in the calculation of the neutron scattering spectrum. Thus we calculate $S(\omega)$ in three steps.

First we treat ferrocene as an isolated purely harmonic molecule. This yields the fundamental vibrational frequencies ω_n and their relative intensities. Here $n=1,\dots,34$, where we apply the nomenclature commonly used in the literature.⁵ Using the resolution of the spectrometer we so obtain the fundamental spectrum $S_f(\omega)$, as shown in Fig. 1(a). Next we include the effect of multiple excitations of ferrocene induced by the incoming neutrons. This yields the spectrum $S_{f,o}(\omega)$ shown in Fig. 1(b). It consists of the fundamental modes ω_n , its overtones, i.e., linear combinations of one ω_n , and their combinations, i.e., linear combinations of different fundamental modes. We observe that there are only minor differences between $S_f(\omega)$ and $S_{f,o}(\omega)$. Virtually none of the very many overtones and combinations can be

TABLE I. The frequencies of the normal modes and their assignment for the present INS experiment and DFT calculations, and the frequencies and assignments from IR and Raman experiments taken from the literature.

Present			Ref. 4	
INS (cm^{-1})	DFT ($\varphi=9^\circ$) (cm^{-1})	Mode #	IR and Raman (cm^{-1})	Mode #
≤ 20	9	6	44	6
180	177	22,21	179	22
315	318	4	309	4
391	395	16	389	16
485	511	11	478	11
504	519	21,22	492	21
598	606	28,34	569	34
			597	28
820–860	800–840	2,9,14,19,27,33	814–855	2,9,14,19
900	876	14,19,25,31	885	33
			897	27
1010	988	13,18	998	13
			1005	18
1060	1026	24,30	1055	31
			1058	25

observed directly (except maybe the one at $\omega=350 \text{ cm}^{-1}$). In practice, the main effect of multiple excitations is that the intensities increase with increasing ω [cf. Figs. 1(a) and 1(b)], due to the increasing number of overtones and combinations.

Finally, we incorporate the effect of the lattice vibrations (phonons) in solid ferrocene. We assume that the phonon spectrum is given by the experimental $S(\omega)$ with $0 \leq \omega \leq 150 \text{ cm}^{-1}$ (cf. Fig. 1). This phonon spectrum is convoluted¹⁴ with the theoretical result $S_{f,o}(\omega)$ to yield $S_{f,o,p}(\omega)$ as shown in Fig. 1(c). One sees that the convolution procedure causes significant sidings in $S_{f,o,p}(\omega)$ to the right of each fundamental peak in $S_{f,o}(\omega)$ [cf. Figs. 1(b) and 1(c)], as has been discussed before.¹⁴

On the basis of the good agreement between the theoretical and experimental spectra in Fig. 1(c) we can, with some confidence, determine the vibrational character of each peak in the experimental spectrum $S(\omega)$.

We start with the six sharp experimental peaks visible at 180, 315, 391, 485, 504, and 598 cm^{-1} . In Table I we compare these values with the present theoretical calculations, from which we derive its character and the labeling according to Ref. 4. In Fig. 3 we give the graphical representations of these vibrational modes: ring-metal-ring bend combined with antisymmetric ring tilt (180 cm^{-1}), metal-ring stretch (315 cm^{-1}), symmetric ring tilt (391 cm^{-1}), metal-ring stretch with oscillating Fe (485 cm^{-1}), antisymmetric ring tilt combined with ring-metal-ring bend (504 cm^{-1}), and out-of-plane ring distortion (combined with CH bending, symmetric and antisymmetric) (598 cm^{-1}). For all these six

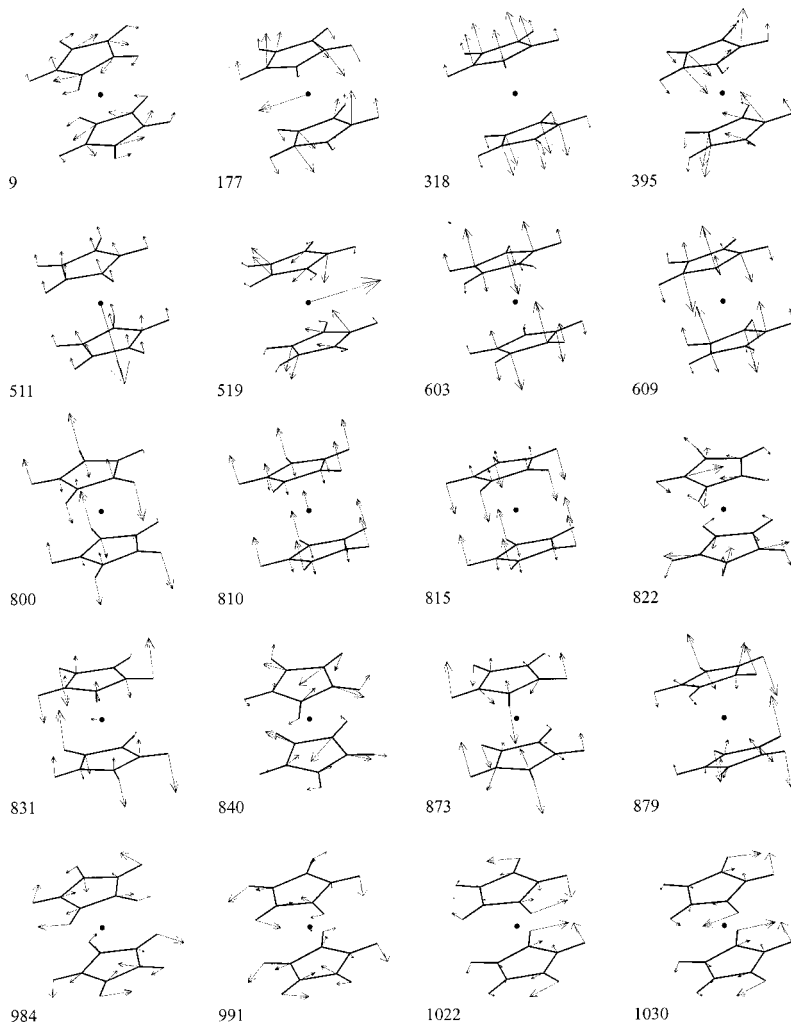


FIG. 3. Graphical representation of the vibrational modes of ferrocene as calculated by DFT. The arrows give the direction and amplitude of the motion of the atoms, the numbers give the calculated frequencies in cm^{-1} .

modes it appears that each H nucleus moves in phase with its nearest C nucleus.

Next, one sees a strong and very broad peak in the measured INS spectrum between ~ 820 and ~ 860 cm^{-1} . We attribute this peak to the contributions of six vibrational modes (also represented in Fig. 3), which are in order of increasing energy in-phase CH bending perpendicular to the ring plane (14), in- and out-of-phase CH bending perpendicular to the ring plane with all the carbon atoms of one ring moving in phase (2 and 9), out-of-phase ring distortion in the ring plane (33), out-of-phase CH bending perpendicular to the ring plane (19), and in-phase ring distortion in the ring plane (27). For these modes it appears that in most cases the H nuclei move out of phase with their nearest C nucleus, but that the CH bond length is fixed.

Then, we assign the sharper isolated peak near 900 cm^{-1} to an in-phase CH bending perpendicular to the ring plane and an out-of-plane ring distortion combined with CH bending. Finally, we attribute the experimental peak at 1010 cm^{-1} to two modes, being respectively, out- and in-phase CH bending in the ring plane and we assign the last clearly visible peak at 1060 cm^{-1} again to CH bending in the ring plane (cf. Table I and Fig. 3).

DISCUSSION

By means of density functional theory we have identified the vibrational character of the most prominent peaks in the INS spectrum of solid ferrocene at 28 K. We start our comparison with results given in the literature with the lowest-lying eigenmode, the so-called torsion mode (number 6 in Ref. 4). Here the two C_5H_5 rings oscillate in plane, but out of phase with each other with frequency ω_6 around the equilibrium position at $\varphi=9^\circ$ (cf. Fig. 3). From our DFT calculations with $\varphi=9^\circ$, we find $\omega_6=9$ cm^{-1} and an intensity as large as that of the peak at 180 cm^{-1} [see Fig. 1(a)]. Therefore this torsion mode falls outside the region $\omega \geq 20$ cm^{-1} covered by our neutron spectrometer. We note, however, that our result $\omega_6=9$ cm^{-1} is extremely sensitive to the equilibrium position φ . By varying φ between 6 and 10 deg we estimate the uncertainty in $\omega_6=9$ cm^{-1} to be at least 100%, i.e., $0 \leq \omega_6 \leq 20$ cm^{-1} . Since we do not see a sharp peak with the correct intensity in the experimental $S(\omega)$ for $\omega > 20$ cm^{-1} , we conclude that the torsion mode frequency must indeed lie in the range $0 \leq \omega_6 \leq 20$ cm^{-1} . In IR spectra a very weak line has been observed at 44 cm^{-1} which has been tentatively attributed to the torsion mode,⁷ while Howard *et al.*⁸ suggested that a peak at 56 cm^{-1} in their inelastic neutron spectrum (at room temperature) might be due to torsion. Our present experiment does not confirm these two expectations. Gardner *et al.*⁹ find in their inelastic neutron spectrum at 5 K a peak at 22 cm^{-1} , and our calculations lend support to their assignment of this peak to the torsion mode.

From our DFT calculations it follows that only the torsion mode frequency ω_6 is sensitive to the equilibration position φ due to the several local minima in the potential barrier as described above. All other frequencies do not change more than a few percent when φ is varied between 0 and 12 deg.

The modes seen in the INS spectrum at 180, 315, 391, 485, and 504 cm^{-1} agree with those given in the literature (see Table I), including their character. We note that the modes at 180 and 504 cm^{-1} are both linear combinations of mode numbers 21 and 22.⁴ This has been suggested before.^{1,6}

In our INS spectrum we do not find a peak at 569 cm^{-1} as reported for IR and Raman spectra, where it is attributed to mode number 34 (cf. Table I and Ref. 4). Instead we find that the modes 28 and 34 yield indistinguishable peaks at 598 cm^{-1} . This confirms the assumption of Lippincott,⁵ based on their character, that both modes have the same frequency. The peak at 569 cm^{-1} , alluded to above, is only actually present in the spectrum shown by Winter *et al.*,¹⁰ who assigned it to mode 34. However, this peak is rather weak and there are several other weak peaks in their IR spectrum, which were left unassigned. It seems likely that these peaks arise from impurities.

The broad INS peak between 820 and 860 cm^{-1} agrees with IR and Raman spectra, including their main character. However, we find that the parallel ring-distortion modes 27 and 33 are included in this INS peak, contrary to what is conjectured for IR and Raman spectra (cf. Table I). Also, we find that the INS peak at 900 cm^{-1} is certainly not due to these modes 27 and 33. Instead, the character is given by orthogonal CH bends with the hydrogens moving out of phase (14,19,25,31, cf. Table I and Fig. 3). The INS peak at 1010 cm^{-1} is due to parallel CH bends (13,18) like in IR and Raman spectra. The INS peak at 1060 cm^{-1} is due to parallel CH bends (24,30) and not to orthogonal CH bends (25,31) as suggested for IR and Raman spectra. In conclusion, we add a new character to the peaks in the spectrum at 900 and 1060 cm^{-1} . We finally note that we have calculated the fundamental modes of an isolated ferrocene molecule which appear to agree reasonably well with those observed in solid ferrocene. Differences might be due to the fact that in solid ferrocene the molecules are not isolated, but interact with each other. Clearly, the low-frequency modes, such as the torsion, will be the most affected. To calculate this interaction from first principles is a formidable task, but it seems feasible in the near future.

¹A. Bércecs, T. Ziegler, and L. Fan, *J. Phys. Chem.* **98**, 1584 (1994).

²P. Seiler and J. D. Dunitz, *Acta Crystallogr., Sect. B: Struct. Crystallogr. Cryst. Chem.* **35**, 2020 (1979).

³A. Haaland and J. E. Nilsson, *Acta Chem. Scand.* **22**, 2653 (1968).

⁴J. S. Bodenheimer and W. Low, *Spectrochim. Acta A* **29**, 1733 (1973).

⁵E. R. Lippincott and R. D. Nelson, *Spectrochim. Acta* **10**, 307 (1958).

⁶E. Diana, R. Rossetti, P. L. Stanghellini, and S. F. A. Kettle, *Inorg. Chem.* **36**, 382 (1997).

⁷F. Rocquet, L. Berreby, and J. P. Marsault, *Spectrochim. Acta A* **29**, 1101 (1973).

⁸J. Howard, T. C. Waddington, and C. J. Wright, *J. Chem. Soc., Faraday Trans. 2* **72**, 513 (1976).

⁹A. B. Gardner, J. Howard, T. C. Waddington, R. M. Richardson, and J. Tomkinson, *Chem. Phys.* **57**, 453 (1981).

¹⁰W. K. Winter, B. Curnutte, Jr., and S. E. Whitcomb, *Spectrochim. Acta* **12**, 1085 (1959).

¹¹K. Palmo and S. Krimm, *J. Comput. Chem.* **19**, 754 (1998).

¹²<http://www.isis.rl.ac.uk/CrystalAnalysers/txa.htm>

¹³B. Delley, *J. Chem. Phys.* **92**, 508 (1990).

¹⁴G. J. Kearley, *Nucl. Instrum. Methods Phys. Res. A* **354**, 53 (1995).